Physica A 488 (2017) 162–176

Contents lists available at ScienceDirect

Physica A

journal homepage: www.elsevier.com/locate/physa

Comparison between different adsorption–desorption kinetics schemes in two dimensional lattice gas

V.J. Huespe [b], R.E. Belardinelli [a,c], V.D. Pereyra [c], S.J. Manzi [a,c,*]

[a] Instituto de Física Aplicada (INFAP) - CONICET, Argentina
[b] Facultad de Ingeniería DETI I, Universidad Nacional de Cuyo, Mendoza, Argentina
[c] Departamento de Física, Universidad Nacional de San Luis, CONICET, Chacabuco 917, 5700 San Luis, Argentina

HIGHLIGHTS

- The influence of the chosen dynamics on the observables obtained from the kinetic lattice gas model is analyzed.
- It is shown that the behavior of the observables depends not only on the lateral interaction, but also on the arbitrarily chosen dynamics.
- Sticking coefficient and TPD spectra are obtained by kinetic Monte Carlo simulation.

ARTICLE INFO

Article history:
Received 11 April 2017
Received in revised form 4 June 2017
Available online 8 July 2017

Keywords:
Dynamic schemes
Sticking coefficient
Programmed thermal desorption spectra
Monte Carlo simulation

ABSTRACT

Monte Carlo simulation is used to study the adsorption–desorption kinetics in the framework of the kinetic lattice-gas model. Three schemes of the so-called hard dynamics and five schemes of the so called soft dynamics were used for this purpose. It is observed that for the hard dynamic schemes, the equilibrium and non-equilibrium observable, such as adsorption isotherms, sticking coefficients, and thermal desorption spectra, have a normal or physical sustainable behavior. While for the soft dynamics schemes, with the exception of the transition state theory, the equilibrium and non-equilibrium observables have several problems.

1. Introduction

Basic research in surface science and interface is highly interdisciplinary, covering the fields of physics, chemistry, biophysics, geographic, atmospheric and environmental sciences, materials science, chemical engineering, among others, specifically the kinetic behavior of the gas–solid interfaces is generally the phenomenon of interest in surface science. The knowledge of the observable behavior, such as sticking coefficient and thermal programmed desorption spectra (TPD), is a particular topic in this area. It is well known that the Arrhenius parameters of the desorption rate constant and the sticking coefficient to be dependent on coverage even in the case of monocrystalline surfaces [1–10]. The coverage dependence of the activation energy for desorption and sticking coefficient is usually attributed to lateral interactions between adsorbed particles or also explained by interactions via precursor states. The coverage dependence of the pre-exponential factor for desorption [9,11] is other interesting problem which not completely understood so far.

The aim of the present paper is to study the influence of different dynamic schemes in the behavior of the adsorption–desorption kinetics in a two-dimensional lattice gas model. Monte Carlo simulations are used to obtain and to analyze the sticking coefficients and TPD spectra which have different behaviors depending on the particular dynamic scheme used.

* Corresponding author at: Departamento de Física, Universidad Nacional de San Luis, CONICET, Chacabuco 917, 5700 San Luis, Argentina.
E-mail address: sergiojmanzi@gmail.com (S.J. Manzi).

http://dx.doi.org/10.1016/j.physa.2017.06.028
0378-4371/

The outline of this work is as follows: In Section 2 the definition of the model and different observable are introduced; In Section 3, the dynamic schemes are introduced and the rate equations which describe the adsorption and desorption processes are derived. In Section 4, the results are presented and discussed. Finally, the conclusions are presented in Section 5.

2. Observables: sticking coefficient and TPD

The theory of the adsorption–desorption kinetics on homogeneous surfaces is by now well understood. One of the methods used in analyzing the problem is the kinetic lattice gas model (KLGM) applied to the adsorbed layer. This method is based on the approximation of the master equation. In the KLGM, adsorption, desorption and diffusion are introduced as Markovian processes through transition probabilities, which must satisfy the detailed balance principle [12–15].

Assuming that the system can be divided into cells, labeled i, for which one introduces microscopic variables $n_{i,j} = 1$ or 0 depending whether cell i is occupied by an adsorbed gas particle or not. To introduce the dynamics of the system one write a model Hamiltonian

$$H = E_s \sum_{i,j} n_{i,j} + V \sum_{nn} n_{i,j} n_{k,l}. \tag{1}$$

The first sum runs over all sites, while the second sum runs over all site pairs whose sites are nearest neighbors (nn). Here E_s is a single particle adsorption energy and V is the two particle interaction between nearest neighbor [16,17].

To describe the temporal behavior of the system, a function $P(\mathbf{n}, t)$ which gives the probability that a given microscopic configuration $\mathbf{n} = \{n_1, n_2, \ldots, n_M\}$ exists at time t is introduced, where M is the total number of adsorption sites on the surface. This probability satisfies a master equation:

$$\frac{dP(\mathbf{n}; t)}{dt} = \sum_{\mathbf{n}'} \left[W(\mathbf{n}; \mathbf{n}') P(\mathbf{n}'; t) - W(\mathbf{n}'; \mathbf{n}) P(\mathbf{n}; t) \right], \tag{2}$$

where $W(\mathbf{n}'; \mathbf{n})$ is the transition probability that the microstate $\mathbf{n}$ changes into $\mathbf{n}'$ per unit time. It satisfies the principle of detailed balance (PDB)

$$W(\mathbf{n}; \mathbf{n}') P_0(\mathbf{n}'; t) = W(\mathbf{n}'; \mathbf{n}) P_0(\mathbf{n}; t). \tag{3}$$

P_0 denotes the equilibrium probability.

Usually, the procedure introduced by Glauber is followed, and guesses of an appropriate form for $W(\mathbf{n}'; \mathbf{n})$ are made. For a two-dimensional lattice gas with nearest-neighbor interactions where only adsorption and desorption processes are taken into account, the transition probability can be written as

$$\begin{aligned} W_{ad-des}(\mathbf{n}'; \mathbf{n}) = & \sum_{\{i,j\}} \{ w_a (1 - n_{i,j}) [A_0 + A_1 (n_{i-1,j} + n_{i+1,j} + n_{i,j-1} + n_{i,j+1}) \\ & + A_2 (n_{i-1,j} n_{i+1,j} + n_{i-1,j} n_{i,j-1} + n_{i-1,j} n_{i,j+1} + n_{i+1,j} n_{i,j-1} + n_{i+1,j} n_{i,j+1} \\ & + n_{i,j-1} n_{i,j+1}) + A_3 (n_{i-1,j} n_{i+1,j} n_{i,j-1} + n_{i-1,j} n_{i+1,j} n_{i,j+1} \\ & + n_{i-1,j} n_{i,j-1} n_{i,j+1} + n_{i+1,j} n_{i,j-1} n_{i,j+1}) + A_4 n_{i-1,j} n_{i+1,j} n_{i,j-1} n_{i,j+1}] \\ & + w_d n_{i,j} [D_0 + D_1 (n_{i-1,j} + n_{i+1,j} + n_{i,j-1} + n_{i,j+1}) \\ & + D_2 (n_{i-1,j} n_{i+1,j} + n_{i-1,j} n_{i,j-1} + n_{i-1,j} n_{i,j+1} + n_{i+1,j} n_{i,j-1} + n_{i+1,j} n_{i,j+1} \\ & + n_{i,j-1} n_{i,j+1}) + D_3 (n_{i-1,j} n_{i+1,j} n_{i,j-1} + n_{i-1,j} n_{i+1,j} n_{i,j+1} \\ & + n_{i-1,j} n_{i,j-1} n_{i,j+1} + n_{i+1,j} n_{i,j-1} n_{i,j+1}) + D_4 n_{i-1,j} n_{i+1,j} n_{i,j-1} n_{i,j+1}] \} \\ & \times \delta (n'_{i,j}, 1 - n_{i,j}) \prod_{\{l,m\} \neq \{i,j\}} \delta (n_{l,m}, n'_{i,j}). \end{aligned} \tag{4}$$

With this, adsorption into site (i, j) occurs if initially $n_{i,j} = 0$, with a rate controlled by prospective neighbors if $A_i \neq 0$. The Kronecker delta for sites $(l, m) \neq (i, j)$ excludes multiple transitions.

The PDB imposes the next set of restrictions on the coefficients A_i and D_i [16–18]

$$w_a (A_0) = w_d (D_0) e^{-\beta E_s}, \tag{5}$$

$$w_a (A_0 + A_1) = w_d (D_0 + D_1) e^{-\beta (E_s + V)}, \tag{6}$$

$$w_a (A_0 + 2A_1 + A_2) = w_d (D_0 + 2D_1 + D_2) e^{-\beta (E_s + 2V)}, \tag{7}$$

$$w_a (A_0 + 3A_1 + 3A_2 + A_3) = w_d (D_0 + 3D_1 + 3D_2 + D_3) e^{-\beta (E_s + 3V)}, \tag{8}$$

$$w_a (A_0 + 4A_1 + 6A_2 + 4A_3 + A_4) = w_d (D_0 + 4D_1 + 6D_2 + 4D_3 + D_4) e^{-\beta (E_s + 4V)}, \tag{9}$$

$\beta = 1/k_B T$, with k_B the Boltzmann's constant. w_a and w_d contain the information about the energy exchange with the solid in the adsorption and desorption processes [16]. PDB provides only half the number of relations to fix these unknown

coefficients in the transition probabilities. Again, the static (lattice-gas) Hamiltonian cannot completely dictate the kind of kinetics possible in the system. As it is pointed out in Refs. [16,17,19–21], any functional relation between the A_i and D_i coefficients must be postulated ad hoc or calculated from a microscopic Hamiltonian that accounts for coupling of the adsorbate to the lattice or electronic degrees of freedom of the substrate. In addition to the PDB, expressions in parentheses of Eqs. (5)–(9) must be greater than zero [17] in order for the dynamic to yield physically correct results. The coverage in KLGM is defined as

$$\theta\left(t\right) = \langle N \rangle = \frac{1}{M} \sum_{s} \sum_{\mathbf{n}} n_s P\left(\mathbf{n}; t\right), \tag{10}$$

where the first sum runs over all (M) sites of the lattice. Considering Eq. (1), the motion equation for coverage can be written as [22–27]:

$$\begin{aligned} \frac{d\theta\left(t\right)}{dt} = {} & w_a \left[A_0 \langle E \rangle + 4A_1 \left\langle \begin{matrix} N \\ E \end{matrix} \right\rangle + 6A_2 \left\langle \begin{matrix} N & N \\ & E \end{matrix} \right\rangle + 4A_3 \left\langle \begin{matrix} N & \\ E & N \\ N & \end{matrix} \right\rangle + A_4 \left\langle \begin{matrix} N & N & \\ & E & N \\ & N & \end{matrix} \right\rangle \right] \\ & - w_d \left[D_0 \langle N \rangle + 4D_1 \left\langle \begin{matrix} N \\ N \end{matrix} \right\rangle + 4D_2 \left\langle \begin{matrix} N & N \\ N & \end{matrix} \right\rangle + 4D_3 \left\langle \begin{matrix} N & \\ N & N \\ N & \end{matrix} \right\rangle + D_4 \left\langle \begin{matrix} N & N & \\ N & N & N \\ & N & \end{matrix} \right\rangle \right]. \end{aligned} \tag{11}$$

$\left\langle \begin{matrix} N \\ E \end{matrix} \right\rangle$ denotes the probability of finding in the lattice the correlation where a site empty have their upper site occupied, and so on with other correlations. After straightforward calculations, this equation can be rewritten as:

$$\begin{aligned} \frac{d\theta\left(t\right)}{dt} = {} & w_a \left[w_{a,0} \left\langle \begin{matrix} & E & \\ E & E & E \\ & E & \end{matrix} \right\rangle + 4w_{a,1} \left\langle \begin{matrix} N & E & E \\ & E & \end{matrix} \right\rangle + 6w_{a,2} \left\langle \begin{matrix} N & N & E \\ & E & \end{matrix} \right\rangle + 4w_{a,3} \left\langle \begin{matrix} N & N & N \\ & E & \end{matrix} \right\rangle \right. \\ & \left. + w_{a,4} \left\langle \begin{matrix} N & N & N \\ & E & \\ & N & \end{matrix} \right\rangle \right] - w_d \left[w_{d,0} \left\langle \begin{matrix} & E & \\ E & N & E \\ & E & \end{matrix} \right\rangle + 4w_{d,1} \left\langle \begin{matrix} N & E & \\ & N & E \\ & E & \end{matrix} \right\rangle \right. \\ & \left. + 6w_{d,2} \left\langle \begin{matrix} N & N & \\ & N & E \\ & E & \end{matrix} \right\rangle + 4w_{d,3} \left\langle \begin{matrix} N & N & N \\ & E & \end{matrix} \right\rangle + w_{d,4} \left\langle \begin{matrix} N & N & N \\ & N & \\ & N & \end{matrix} \right\rangle \right], \end{aligned} \tag{12}$$

where

$$A_0 = w_{a,0}, \tag{13}$$

$$A_0 + A_1 = w_{a,1}, \tag{14}$$

$$A_0 + 2A_1 + A_2 = w_{a,2}, \tag{15}$$

$$A_0 + 3A_1 + 3A_2 + A_3 = w_{a,3}, \tag{16}$$

$$A_0 + 4A_1 + 6A_2 + 4A_3 + A_4 = w_{a,4}, \tag{17}$$

$$D_0 = w_{d,0}, \tag{18}$$

$$D_0 + D_1 = w_{d,1}, \tag{19}$$

$$D_0 + 2D_1 + D_2 = w_{d,2}, \tag{20}$$

$$D_0 + 3D_1 + 3D_2 + D_3 = w_{d,3}, \tag{21}$$

$$D_0 + 4D_1 + 6D_2 + 4D_3 + D_4 = w_{d,4}. \tag{22}$$

$w_{a,i}$ $\left(w_{d,i}\right)$ corresponding to the adsorption (desorption) probability of a particle in a particular site of the lattice which have their i nearest neighbor sites occupied.

2.1. Sticking coefficient

Alternatively to the master equation treatment, the rate equation for coverage can be written through of the phenomenological formulation, as a difference between adsorption and desorption terms:

$$\frac{d\theta}{dt} = R_a - R_d. \tag{23}$$

The adsorption term can be specified as a product of the particles flow that reaches the surface from gas phase with pressure P and temperature T, hitting the area a_s of an adsorption cell, and adsorbing with a probability equal to $S(\theta, T)$, i.e.:

$$R_a = S(\theta, T)\,\frac{a_s P \lambda}{h}. \tag{24}$$

$S(\theta, T)$ is called the sticking coefficient [16,17], λ is the thermal wavelength, and h is the Planck's constant. Sticking coefficient cannot be obtained by thermodynamic arguments and must be calculated from a microscopic theory or postulated from a phenomenological approach based on experimental evidence for a particular system.

Considering that $w_a = w_d = w_0$, and by comparison with the phenomenological expression for adsorption [28], one can identify it as

$$w_0 = S_0(T)\,\frac{a_s P \lambda}{h}, \tag{25}$$

where $S_0(T)$ is the temperature-dependent sticking coefficient at zero coverage.

From the rate equation for coverage (Eq. (12)), the sticking coefficient in a square lattice with nearest neighbor interaction is [16,17,29,30]:

$$\begin{aligned} S(\theta, T) = {} & A_0 \left\langle \begin{matrix} & E & \\ E & E & E \\ & E & \end{matrix} \right\rangle + 4(A_0 + A_1) \left\langle \begin{matrix} & E & \\ N & E & E \\ & E & \end{matrix} \right\rangle + 6(A_0 + 2A_1 + A_2) \left\langle \begin{matrix} & N & \\ & E & E \\ & E & \end{matrix} \right\rangle \\ & + 4(A_0 + 3A_1 + 3A_2 + A_3) \left\langle \begin{matrix} & N & \\ N & E & N \\ & E & \end{matrix} \right\rangle + (A_0 + 4A_1 + 6A_2 + 4A_3 + A_4) \left\langle \begin{matrix} & N & \\ & E & N \\ & N & \end{matrix} \right\rangle. \end{aligned} \tag{26}$$

2.2. Thermal programmed desorption spectra

Thermal desorption is one of the most important experimental techniques to study the properties of the adsorbed layer on solid surfaces through the determination of kinetic and thermodynamic parameters of the desorption process. Analyzes of this type provide very useful information for understanding the mechanisms involved in the processes occurring in the system, when the spectra are analyzed using appropriate models. This can be done by simulation techniques and different kinetic Monte Carlo approaches, which have proven to give satisfactory results in the interpretation of thermal desorption experiments on surfaces [6,24,31].

Thermal desorption can be studied from the kinetic equations, annulling the adsorption process and letting the system evolve. Thus it is possible to change surface coverage versus time. Considering a dependence between time and temperature, it is possible to obtain desorption spectra depending on the temperature. When the proposed dependence is linear, the proportionality constant is called heating rate. In this paper two cases of thermal desorption, depending on whether the adsorbate remains mobile or immobile, are going to be studied. For mobile adsorbate, it is considered that during desorption the diffusion process is faster than the other processes involved. Under this condition, the adsorbate remain in a state of quasi-equilibrium during desorption [4].

For a mobile TPD, it should be allowed that the system is always in equilibrium. In general, it is assumed that the desorption is an activated process.

3. Dynamic schemes

The choice of dynamic scheme in the description of surface processes is very important. Such schemes can be classified into non-conservative dynamic or soft (soft dynamic), in which the transition probabilities can be factored into a dependent term of the energies of lateral interaction and other energy-dependent field and conservative dynamic or hard (hard dynamic) where such factorization is not possible. For calculating sticking coefficient and TPD, it is imperative to know the adsorption (A_i) and desorption (D_i) coefficients.

3.1. Soft dynamics

3.1.1. Interaction kinetics

This scheme was introduced by Payne and Kreuzer [12,16,20,21], assuming a linear relation between the adsorption and desorption coefficients:

$$\frac{A_i}{A_0} = \gamma \frac{D_i}{D_0}, \tag{27}$$

where γ is a proportional coefficient, and usually $A_0 = 1$. The PDB imposes that the adsorption and desorption coefficients for two dimensional lattice gas are given by

$$A_1 = \gamma \left(\frac{e^{\beta V} - 1}{1 - \gamma e^{\beta V}} \right), \tag{28}$$

$$A_2 = \gamma\left(\frac{e^{2\beta V}-1}{1-\gamma e^{2\beta V}}\right) - 2A_1, \tag{29}$$

$$A_3 = \gamma\left(\frac{e^{3\beta V}-1}{1-\gamma e^{3\beta V}}\right) - 3A_1 - 3A_2, \tag{30}$$

$$A_4 = \gamma\left(\frac{e^{4\beta V}-1}{1-\gamma e^{4\beta V}}\right) - 4A_1 - 6A_2 - 4A_3, \tag{31}$$

$$D_0 = e^{\beta E_s}, \tag{32}$$

$$D_1 = D_0\left(\frac{e^{\beta V}-1}{1-\gamma e^{\beta V}}\right), \tag{33}$$

$$D_2 = D_0\left(\frac{e^{2\beta V}-1}{1-\gamma e^{2\beta V}}\right) - 2D_1, \tag{34}$$

$$D_3 = D_0\left(\frac{e^{3\beta V}-1}{1-\gamma e^{3\beta V}}\right) - 3D_1 - 3D_2, \tag{35}$$

$$D_4 = D_0\left(\frac{e^{4\beta V}-1}{1-\gamma e^{4\beta V}}\right) - 4D_1 - 6D_2 - 4D_3. \tag{36}$$

3.1.2. Transition state theory (TST)

The TST provides a way to obtain the constant rates of the involved processes through the knowledge of the appropriate kinetic equations [17,18,32–37]. For a two dimensional KLGM with nearest neighbor lateral interaction, the corresponding adsorption and desorption coefficients are given by:

$$A_0 = e^{-\beta\left(\frac{E_s}{2}+\epsilon_0^*\right)}, \tag{37}$$

$$A_1 = e^{-\beta\frac{E_s}{2}}\left(e^{-\beta\epsilon_1^*} - e^{-\beta\epsilon_0^*}\right), \tag{38}$$

$$A_2 = e^{-\beta\frac{E_s}{2}}\left(e^{-\beta\epsilon_2^*} - 2e^{-\beta\epsilon_1^*} + e^{-\beta\epsilon_0^*}\right), \tag{39}$$

$$A_3 = e^{-\beta\frac{E_s}{2}}\left(e^{-\beta\epsilon_3^*} - 3e^{-\beta\epsilon_2^*} - 3e^{-\beta\epsilon_1^*} + e^{-\beta\epsilon_0^*}\right), \tag{40}$$

$$A_4 = e^{-\beta\frac{E_s}{2}}\left(e^{-\beta\epsilon_4^*} - 4e^{-\beta\epsilon_3^*} - 6e^{-\beta\epsilon_2^*} - 4e^{-\beta\epsilon_1^*} + e^{-\beta\epsilon_0^*}\right), \tag{41}$$

$$D_0 = e^{\beta\left(\frac{E_s}{2}-(\epsilon_0^*-\epsilon_0)\right)}, \tag{42}$$

$$D_1 = e^{\beta\frac{E_s}{2}}\left(e^{-\beta(\epsilon_1^*-\epsilon_1)} - e^{-\beta(\epsilon_0^*-\epsilon_0)}\right), \tag{43}$$

$$D_2 = e^{\beta\frac{E_s}{2}}\left(e^{-\beta(\epsilon_2^*-\epsilon_2)} - 2e^{-\beta(\epsilon_1^*-\epsilon_1)} + e^{-\beta(\epsilon_0^*-\epsilon_0)}\right), \tag{44}$$

$$D_3 = e^{\beta\frac{E_s}{2}}\left(e^{-\beta(\epsilon_3^*-\epsilon_3)} - 3e^{-\beta(\epsilon_2^*-\epsilon_2)} - 3e^{-\beta(\epsilon_1^*-\epsilon_1)} + e^{-\beta(\epsilon_0^*-\epsilon_0)}\right), \tag{45}$$

$$D_4 = e^{\beta\frac{E_s}{2}}\left(e^{-\beta(\epsilon_4^*-\epsilon_4)} - 4e^{-\beta(\epsilon_3^*-\epsilon_3)} - 6e^{-\beta(\epsilon_2^*-\epsilon_2)} - 4e^{-\beta(\epsilon_1^*-\epsilon_1)} + e^{-\beta(\epsilon_0^*-\epsilon_0)}\right). \tag{46}$$

where ϵ_i and ϵ_i^* are the lateral interactions (with i first neighbors occupied) in the initial state (or base) and activated (or transition) state, respectively. If the Brönsted–Polanyi relation for interaction energies in initial and final state [17,38] is considered, the coefficients reduce to:

$$A_i = e^{-\beta\frac{E_s}{2}}\left(e^{-\beta\frac{V}{2}} - 1\right)^i, \tag{47}$$

$$D_i = e^{\beta\frac{E_s}{2}}\left(e^{\beta\frac{V}{2}} - 1\right)^i, \tag{48}$$

with $i = 1, 2, 3, 4$.

3.1.3. Inverse relation

The adsorption and desorption coefficients defined by

$$A_i = e^{-\beta\left(\frac{E_s}{2}+iV\right)}, \tag{49}$$

$$D_i = e^{\beta\left(\frac{E_s}{2}+iV\right)}, \tag{50}$$

where $i = 1, 2, 3, 4$, fulfill the PDB for two dimensional lattice gas with nearest neighbor lateral interaction.

3.1.4. Soft Glauber

In this scheme, the adsorption and desorption coefficients take the following forms:

$$A_0 = \left(\frac{1}{1+e^{\beta E_s}}\right), \tag{51}$$

$$A_1 = \frac{e^{-\beta V}}{\left(1+e^{\beta E_s}\right)\left(1+e^{\beta V}\right)}, \tag{52}$$

$$A_2 = \frac{e^{\beta V}\left(2-e^{\beta V}+e^{2\beta V}\right)}{\left(1+e^{\beta E_s}\right)\left(1+e^{\beta V}\right)\left(1+e^{2\beta V}\right)}, \tag{53}$$

$$A_3 = \frac{-e^{\beta V}\left(3-6e^{\beta V}+7e^{2\beta V}-3e^{3\beta V}+e^{4\beta V}\right)}{\left(1+e^{\beta E_s}\right)\left(1+e^{2\beta V}\right)\left(1+e^{3\beta V}\right)}, \tag{54}$$

$$A_4 = \frac{e^{\beta V}\left(4-10e^{\beta V}+12e^{2\beta V}-5e^{3\beta V}+6e^{4\beta V}-11e^{5\beta V}+11e^{6\beta V}-4e^{7\beta V}+e^{8\beta V}\right)}{\left(1+e^{\beta E_s}\right)\left(1+e^{2\beta V}\right)\left(1+e^{3\beta V}\right)\left(1+e^{4\beta V}\right)}, \tag{55}$$

$$D_0 = \left(\frac{1}{1+e^{-\beta E_s}}\right), \tag{56}$$

$$D_1 = \frac{-e^{-\beta V}}{\left(1+e^{-\beta E_s}\right)\left(1+e^{-\beta V}\right)}, \tag{57}$$

$$D_2 = \frac{e^{-\beta V}\left(2-e^{-\beta V}+e^{-2\beta V}\right)}{\left(1+e^{-\beta E_s}\right)\left(1+e^{-\beta V}\right)\left(1+e^{-2\beta V}\right)}, \tag{58}$$

$$D_3 = \frac{-e^{-\beta V}\left(3-6e^{-\beta V}+7e^{-2\beta V}-3e^{-3\beta V}+e^{-4\beta V}\right)}{\left(1+e^{-\beta E_s}\right)\left(1+e^{-2\beta V}\right)\left(1+e^{-3\beta V}\right)}, \tag{59}$$

$$D_4 = \frac{e^{-\beta V}\left(4-10e^{-\beta V}+12e^{-2\beta V}-5e^{-3\beta V}+6e^{-4\beta V}-11e^{-5\beta V}+11e^{-6\beta V}-4e^{-7\beta V}+e^{-8\beta V}\right)}{\left(1+e^{-\beta E_s}\right)\left(1+e^{-2\beta V}\right)\left(1+e^{-3\beta V}\right)\left(1+e^{-4\beta V}\right)}. \tag{60}$$

3.1.5. One step dynamic (OSD)

The adsorption and desorption coefficients are

$$A_i = e^{-\beta U}e^{-\beta\frac{E_s}{2}}\left(e^{-\beta\frac{V}{2}}-1\right)^i, \tag{61}$$

$$D_i = e^{-\beta U}e^{\beta\frac{E_s}{2}}\left(e^{\beta\frac{V}{2}}-1\right)^i, \tag{62}$$

respectively. Here, i determines the amount of occupied nearest neighbor sites, and U is the energy barrier between final and initial state. Note that when $U = 0$, this dynamic scheme gets the same results as those obtained by applying the relationship Brönsted–Polanyi in TST scheme.

3.2. Hard dynamics

3.2.1. Two-steps transition dynamic approximation (TDA)

Introduced to explain different problems in surface science [17,19,39–41], the adsorption and desorption coefficients are given by

$$A_0 = \left(\frac{1}{1+e^{\beta\left(\frac{E_s}{2}+U\right)}}\right)\left(\frac{1}{1+e^{\beta\left(\frac{E_s}{2}-U\right)}}\right), \tag{63}$$

$$A_1 = \left(\frac{1}{1+e^{\beta\left(\frac{E_s+V}{2}+U\right)}}\right)\left(\frac{1}{1+e^{\beta\left(\frac{E_s+V}{2}-U\right)}}\right) - A_0, \tag{64}$$

$$A_2 = \left(\frac{1}{1+e^{\beta\left(\frac{E_s+2V}{2}+U\right)}}\right)\left(\frac{1}{1+e^{\beta\left(\frac{E_s+2V}{2}-U\right)}}\right) - 2A_1 - A_0, \tag{65}$$

$$A_3 = \left(\frac{1}{1+e^{\beta\left(\frac{E_s+3V}{2}+U\right)}}\right)\left(\frac{1}{1+e^{\beta\left(\frac{E_s+3V}{2}-U\right)}}\right) - 3A_2 - 3A_1 - A_0, \tag{66}$$

$$A_4 = \left(\frac{1}{1+e^{\beta\left(\frac{E_s+4V}{2}+U\right)}}\right)\left(\frac{1}{1+e^{\beta\left(\frac{E_s+4V}{2}-U\right)}}\right) - 4A_3 - 6A_2 - 4A_1 - A_0, \tag{67}$$

$$D_0 = \left(\frac{1}{1+e^{-\beta\left(\frac{E_s}{2}+U\right)}}\right)\left(\frac{1}{1+e^{-\beta\left(\frac{E_s}{2}-U\right)}}\right), \tag{68}$$

$$D_1 = \left(\frac{1}{1+e^{-\beta\left(\frac{E_s+V}{2}+U\right)}}\right)\left(\frac{1}{1+e^{-\beta\left(\frac{E_s+V}{2}-U\right)}}\right) - D_0, \tag{69}$$

$$D_2 = \left(\frac{1}{1+e^{-\beta\left(\frac{E_s+2V}{2}+U\right)}}\right)\left(\frac{1}{1+e^{-\beta\left(\frac{E_s+2V}{2}-U\right)}}\right) - 2D_1 - D_0, \tag{70}$$

$$D_3 = \left(\frac{1}{1+e^{-\beta\left(\frac{E_s+3V}{2}+U\right)}}\right)\left(\frac{1}{1+e^{-\beta\left(\frac{E_s+3V}{2}-U\right)}}\right) - 3D_2 - 3D_1 - D_0, \tag{71}$$

$$D_4 = \left(\frac{1}{1+e^{-\beta\left(\frac{E_s+4V}{2}+U\right)}}\right)\left(\frac{1}{1+e^{-\beta\left(\frac{E_s+4V}{2}-U\right)}}\right) - 4D_3 - 6D_2 - 4D_1 - D_0. \tag{72}$$

3.2.2. Ising kinetics

Considering the next relations between adsorption and desorption coefficients [20]:

$$A_i = \gamma D_i, \tag{73}$$

with $i = 1, 2, 3, 4$ and considering $A_0 = 1$, PDB gives the next expressions for desorption coefficients:

$$D_0 = e^{\beta E_s}, \tag{74}$$

$$D_1 = D_0\left(\frac{e^{\beta V}-1}{1-\gamma D_0 e^{\beta V}}\right), \tag{75}$$

$$D_2 = D_0\left(\frac{e^{2\beta V}-1}{1-\gamma D_0 e^{2\beta V}}\right) - 2D_1, \tag{76}$$

$$D_3 = D_0\left(\frac{e^{3\beta V}-1}{1-\gamma D_0 e^{3\beta V}}\right) - 3D_1 - 3D_2, \tag{77}$$

$$D_4 = D_0\left(\frac{e^{4\beta V}-1}{1-\gamma D_0 e^{4\beta V}}\right) - 4D_1 - 6D_2 - 4D_3. \tag{78}$$

3.2.3. Standard Glauber dynamics

This dynamic scheme is one of the most well known and widely used [42], and their corresponding adsorption and desorption coefficients are given by:

$$A_0 = \left(\frac{1}{1+e^{\beta E_s}}\right), \tag{79}$$

$$A_1 = \left(\frac{1}{1+e^{\beta(E_s+V)}}\right) - A_0, \tag{80}$$

$$A_2 = \left(\frac{1}{1+e^{\beta(E_s+2V)}}\right) - 2A_1 - A_0, \tag{81}$$

$$A_3 = \left(\frac{1}{1+e^{\beta(E_s+3V)}}\right) - 3A_2 - 3A_1 - A_0, \tag{82}$$

$$A_4 = \left(\frac{1}{1+e^{\beta(E_s+4V)}}\right) - 4A_3 - 6A_2 - 4A_1 - A_0, \tag{83}$$

$$D_0 = \left(\frac{1}{1+e^{-\beta E_s}}\right), \tag{84}$$

$$D_1 = \left(\frac{1}{1+e^{-\beta(E_s+V)}}\right) - D_0, \tag{85}$$

$$D_2 = \left(\frac{1}{1+e^{-\beta(E_s+2V)}}\right) - 2D_1 - D_0, \tag{86}$$

$$D_3 = \left(\frac{1}{1+e^{-\beta(E_s+3V)}}\right) - 3D_2 - 3D_1 - D_0, \tag{87}$$

$$D_4 = \left(\frac{1}{1+e^{-\beta(E_s+4V)}}\right) - 4D_3 - 6D_2 - 4D_1 - D_0. \tag{88}$$

Note that, using Eqs. (13)–(22), it is possible to obtain the adsorption and desorption probabilities for each dynamic scheme.

4. Results

The results are obtained doing Monte Carlo simulations in 120 × 120 square lattices with periodic boundary conditions. To evaluate sticking coefficient the simulations are carried out in Grand Canonical Ensemble, where each point is the average over 10^6 Monte Carlo step (MCS). To obtain TPD spectra, a *n*-Fold way algorithm is used [43]. In these simulations, an initial thermalization at low temperature is carried out over 10^6 MCS, and final spectrum is the average over 1000 independent spectra. In all TPD simulations the adsorption is considered as an activated process, with an activation energy of 25 kcal/mol, a pre-exponential factor of 10^{10} s^{-1}, an initial coverage $\theta_0 = 0.9$, and a heating rate of 1 K/s.

4.1. Sticking coefficient

4.1.1. Soft dynamics

In Fig. 1 the normalized sticking coefficient for different dynamic schemes and values of the lateral interaction is showed. In the interaction kinetics, as Fig. 1(a) shows, for repulsive lateral interactions all curves are below for non-interacting curve ($V = 0$, dashed line in Fig. 1) $S(\theta,T)/S(0,T) = (1-\theta)$. For $\beta V \gg 0$: $\frac{A_1}{A_0} \to -1$, $\frac{A_2}{A_0} \to 1$, $\frac{A_3}{A_0} \to -1$ and $\frac{A_4}{A_0} \to 1$, then $S(\theta,T)/S(0,T)$ is independent of γ, and it is given by the correlation $\left\langle \begin{matrix} & E & \\ E & E & E \\ & E & \end{matrix} \right\rangle$. With increasing coverage, this correlation fell sharply and thus also the sticking coefficient. When the lateral interaction grows in positive values (attractive lateral interaction), the normalized sticking coefficient reaches a limit curve and then decrease to limit curve $(1-\theta)$. This is, the normalized sticking coefficient shows the same behavior both null lateral interaction as large attractive lateral interaction. Taking account that the sticking coefficient is proportional to the first parenthesis in Eq. (11), and that for $\beta V \ll 0$, $\left\langle \begin{matrix} N \\ N \end{matrix} \right\rangle \to \theta$, $\left\langle \begin{matrix} N \\ E \end{matrix} \right\rangle \to 0$, adding that all ratios A_i/A_0 are finite, then this scheme gives a normalized sticking coefficient equal to $(1-\theta)$ for large attractive lateral interaction.

In Fig. 1(b), the sticking coefficient for TST is shown. For large repulsive lateral interaction the behavior is similar to the Interaction Kinetics. While for attractive lateral interaction, sticking coefficient growth monotonically with it (ratios $\frac{A_i}{A_0} \to \infty$ for $\beta V \ll 0$). For $V = 0$, the expected behavior $S(\theta,T)/S(0,T) = (1-\theta)$ is obtained, agree that the sticking probability depends only on the probability of an empty site to be found.

In Fig. 1(c) the normalized sticking coefficient for Inverse Relation kinetics, with different values of the lateral interaction is shown. For $V = 0$, all ratios $A_i/A_0 = 1$, and taking into account that the coverage of each site is independent of the coverage of their nearest neighbor sites, therefore each correlation in Eq. (26) can be replaced by the product $\theta^s(1-\theta)^r$, where s (r) is the number of occupied (empty) sites in the corresponding correlation. With this, the normalized sticking coefficient for non-interacting case can be expressed by:

$$\frac{S(\theta,T)}{S(0,T)} = (1-\theta)\left[1+4\theta+6\theta^2+4\theta^3+\theta^4\right]. \tag{89}$$

Note that this expression differs of the normal behavior for null interaction (should be proportional to $(1-\theta)$). For attractive lateral interaction, normalized sticking coefficient increases with the increasing of the interaction. For large repulsive lateral interaction all coefficients A_i converge to the same value of A_0, whereby the normalized sticking coefficient ranges from Eq. (89) to $(1-\theta)$ with the increasing of the lateral interaction.

In Soft Glauber dynamic scheme, the normalized sticking coefficient converge to upper limit curve $(1-\theta)$ for large attractive lateral interaction (see Fig. 1(d)). In order to explain this, for $\beta V \to -\infty$ the adsorption coefficients $\frac{A_i}{A_0} \to 0$ given the proposed limit for sticking coefficient. For $V = 0$, adsorption coefficients are $\frac{A_1}{A_0} = \frac{A_3}{A_0} = -\frac{1}{2}$ and $\frac{A_2}{A_0} = \frac{A_4}{A_0} = \frac{1}{2}$, and considering that the occupation of a site is independent of their neighboring, the normalized sticking coefficient for null interaction is:

$$\frac{S(\theta,T)}{S(0,T)} = (1-\theta)\left[1-2\theta+3\theta^2-2\theta^3+\frac{1}{2}\theta^4\right]. \tag{90}$$

Normalized sticking coefficient decreases from this curve with increasing repulsive lateral interaction. Regardless of the value of U, the sticking coefficient normalized to the OSD has the same behavior as that obtained by the TST. The sticking

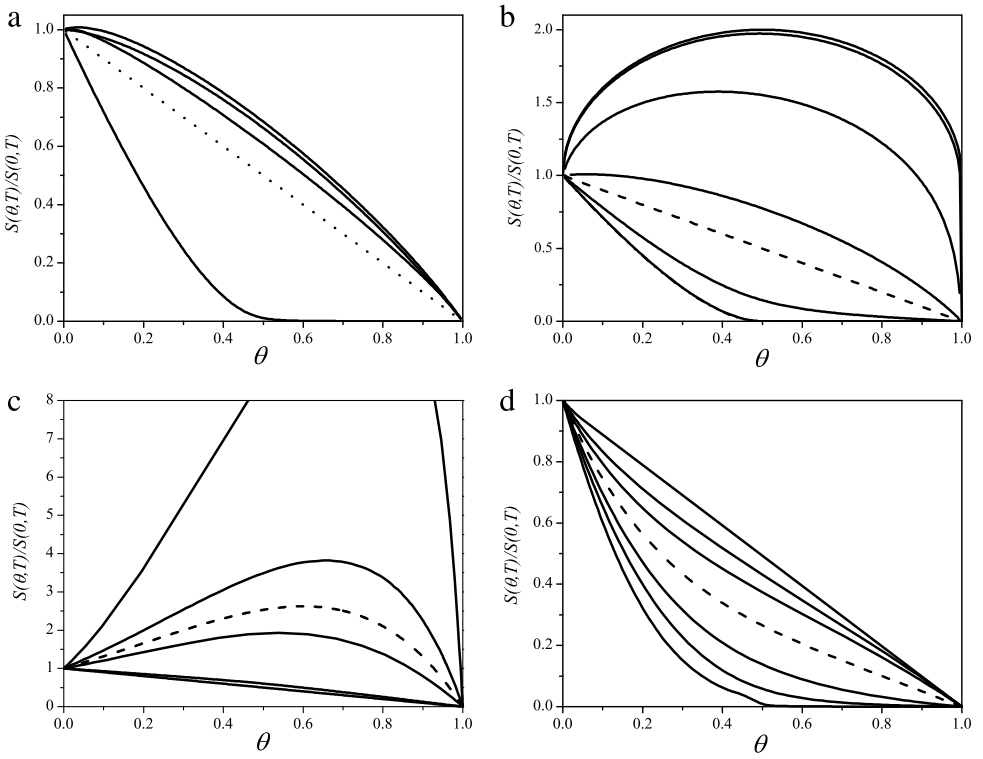

Fig. 1. Normalized sticking coefficient as a function of coverage θ for soft dynamics. (a) Interaction kinetic, bottom to top at $\theta = 0.5$, $\beta V = 3, 0, -4, -1, -2$; (b) TST: bottom to top $\beta V = 10, 2, 0, -1, -4, -10, -20$; (c) Inverse relation: bottom to top $\beta V = 2, 1, 0.3, 0, -0.3, -1$; (d) Soft Glauber: bottom to top $\beta V = 2, 1, 0.5, 0, -0.5, -1, -2$.

coefficient calculated with the standard Glauber dynamics presents the same behavior that the corresponding to the Ising dynamic.

4.1.2. Hard dynamics

As seen in Fig. 2(a), the normalized coefficient sticking for Ising kinetics increases with increasing attractive lateral interaction, while it decreases for repulsive lateral interaction. The minimum in sticking coefficient is due to when the system is in the ordered phase $c(2 \times 2)$ the adsorption of new particles is not allowed until the chemical potential growths enough so that new particles can be adsorbed in the system (In hard dynamics, sticking coefficient depends on chemical potential.). From repulsive lateral interactions $\beta V = 4$ no differences were observed in the sticking coefficient. When lateral interaction is equal to zero, the expected dependence $(1 - \theta)$ is obtained. The normalized sticking coefficient for the TDA is shown in Fig. 2(b) and (c) for a fixed value of the transition state energy U, the behavior of $S(\theta, T)/S(0, T)$ can be explained as follows. As the lateral interaction increases, the normalized sticking coefficient increases monotonically in the range, $0 < \theta < 1$, dropping to zero at monolayer. This occurs because all ratios A_i/A_0 diverge for large attraction lateral interaction ($\beta V \ll 0$). For large repulsive lateral interaction ($\beta V \gg 0$) and coverages $\theta < \frac{1}{2}$, we have the following limits for the ratios $\frac{A_1}{A_0} \to -1$, $\frac{A_3}{A_0} \to -1$ and $\frac{A_2}{A_0} \to 1$, $\frac{A_4}{A_0} \to 1$, making the normalized sticking coefficient reaches a limit curve (this is because $\left\langle \begin{matrix} & N & \\ N & E & N \\ & N & \end{matrix} \right\rangle \to 0$).

4.2. Thermal programmed desorption spectra

4.2.1. Soft dynamics

Figs. 3–7 show TPD spectra for soft dynamics, in all spectra initial coverage is $\theta_0 = 0.9$. In Fig. 3 TPD spectra for Interaction Kinetics with $\gamma = -1$ and different values of the lateral interaction are shown. For attractive lateral interaction the temperature of the peaks shifts to higher temperatures for immobile adsorbate. This is due to the mobility disperses particles in the lattice by decreasing desorption energy, so they leave the surface at lower temperatures. The mobile TPD is formed from those particles desorbing with one, two, and no-nearest neighbor sites occupied, while the immobile case is formed almost exclusively from particles with two nearest neighbors occupied, which come from the edge of single cluster which decreases in size during desorption. For repulsive lateral interaction, TPD spectra present a weak dependence with

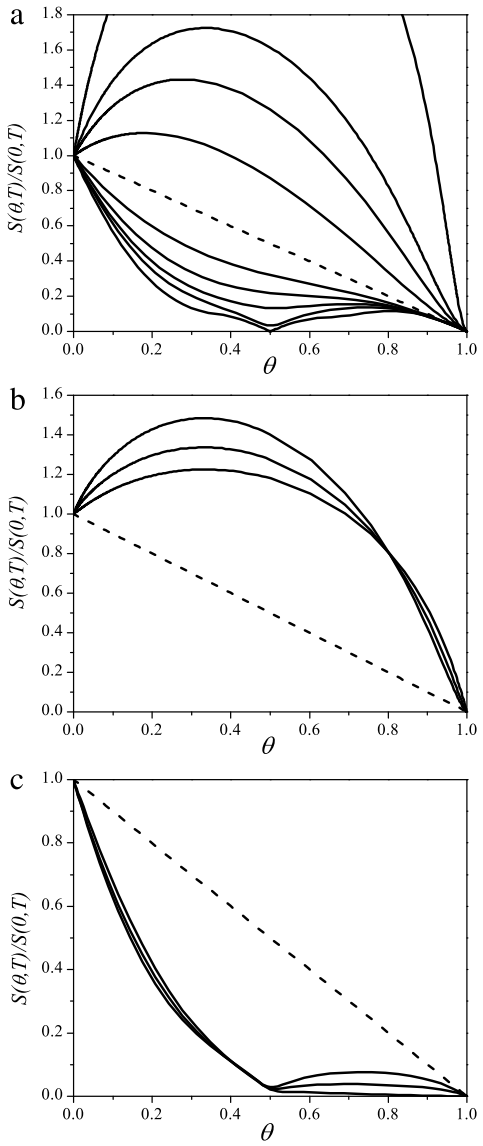

Fig. 2. Normalized sticking coefficient as a function of coverage θ for hard dynamics. (a) Ising kinetic, bottom to top $\beta V = 6, 2, 1.5, 1, 0.5, 0, -0.5, -0.8, -1, -1.5$; (b) TDA: bottom to top at $\theta = 0.5$, $\beta V = 0, -1(\beta U = 10), -1(\beta U = 2), -1(\beta U = 0)$; (c) TDA: bottom to top at $\theta = 0.8$, $\beta V = 2(\beta U = 10), -1(\beta U = 2), -1(\beta U = 0), 0$.

it, reaching a limit curve when $V \sim 4$ kcal/mol. Note that the desorption coefficients D_i are independent of V for large values of V (see Eqs. (32)–(36)). Here, the double peak for the mobile case can be explained through the surface order of adsorbate due to lateral repulsive interaction. While for the immobile case, this ordered structure is not observed. TPD spectra for TST dynamic are shown in Fig. 4. For attractive lateral interaction, the peak of the immobile TPD has a lower temperature than mobile TPD. Note that both TPD have the same beginning. In the immobile case appear particles with different amount of occupied nearest neighbor sites, while adsorbate can be realign in a compact cluster for the mobile TPD, requiring higher temperature for desorb. When lateral interaction is repulsive, the immobile TPD spectra present five peaks (provided that the initial coverage is greater than 0.5). They are made sharper at higher values of the lateral interaction. The lower temperature peak corresponds to those particles that desorb and have their four nearest neighbor sites occupied. The next peak, is formed by the desorbing particles with three nearest neighbor sites occupied, and so on for other peaks. The higher temperature peak is formed by desorbing isolated particles, note that this peak temperature is the same as for the non-interacting TPD spectrum. Mobile TPD spectra present only two peaks (again, initial coverage must be greater than 0.5). The highest temperature peak is formed by desorbing particles with their four nearest neighbor sites occupied, the valley between peaks (there are not desorbing particles) evidences an ordered structure ($c(2 \times 2)$ phase) where the adsorbate

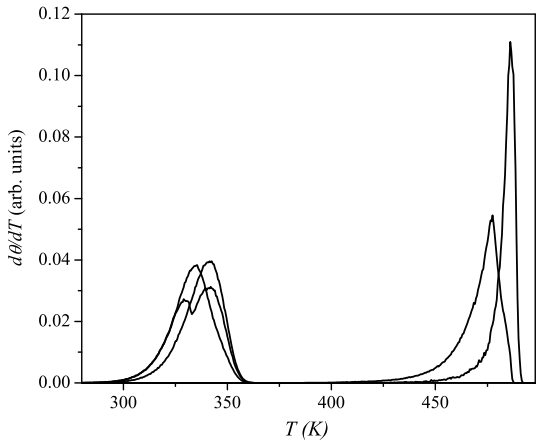

Fig. 3. TPD spectra as a function of temperature T for Interaction Kinetics with initial coverage $\theta_0 = 0.9$. From right to left V (kcal/mol) $= -4$ (immobile), -4 (mobile), 0, 2 (mobile), 2 (immobile).

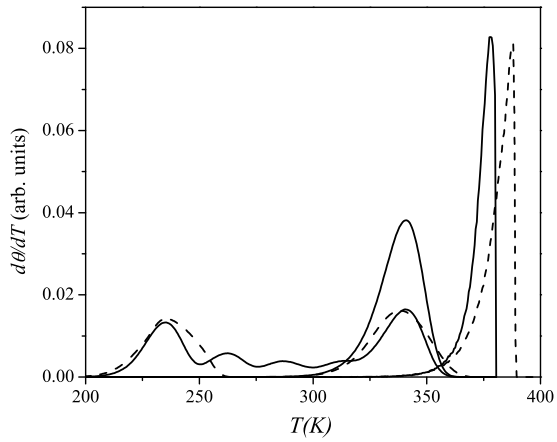

Fig. 4. Mobile (dash line) and immobile (line) TPD spectra as a function of temperature T for TST dynamic with initial coverage $\theta_0 = 0.9$ and different values of the lateral interaction, left to right V (kcal/mol) $= 4, 0, -2$. For $V = 0$, mobile and immobile spectra coincide.

like a chessboard. Finally, the highest temperature peak is, principally, due to those isolated particles that desorb from lattice.

The TPD spectra for Inverse Relation scheme are shown in Fig. 5. For repulsive lateral interaction, TPD spectra present the same behavior as the TST dynamic. When lateral interaction is null, the mobile and immobile TPD do not match. Explicitly, writing Eq. (12) without adsorption term for this scheme with $V = 0$, desorption rate depends on amount of nearest neighbor occupied sites. While for the mobile TPD this amount is a function of the coverage; for the immobile TPD there is a greater amount of isolated particles which they need more temperature for desorb due to their greater desorption energy and they form the last part of the spectrum. For attractive lateral interaction, TPD spectra shift to higher temperature only slightly, and for upper of 3 kcal/mol, they are independent of the lateral interaction and the mobility. This last can be deduced making $V \to -\infty$ in Eqs. (18)–(22), and taking account Eqs. (48). Fig. 6 shows TPD spectra for Soft Glauber Dynamic. The main characteristic of these TPD is that immobile and mobile TPD spectra does not match for non-interacting case. Both large attractive and large repulsive lateral interactions, TPD spectra does not show any difference. The Fig. 7 shows the effect of U on immobile TPD spectra for One-Step Dynamic with repulsive lateral interaction. The temperature difference between the last and first peaks is independent on U. This energy barrier U shifts the whole spectra to lower (higher) temperatures when their value is negative (positive). In this case, the number of the peaks does not changes, except that the peaks become wider with temperature, overlapping on each other. For the attractive lateral interactions, the shifting of the spectra with U have similar behavior that repulsive lateral interaction.

4.2.2. Hard dynamics

Thermal desorption spectra for hard dynamics are shown in Figs. 8 and 9. In the Ising kinetic, the immobile spectrum presents the five characteristic peaks corresponding to the number of neighbors occupied by the desorbing particle, which

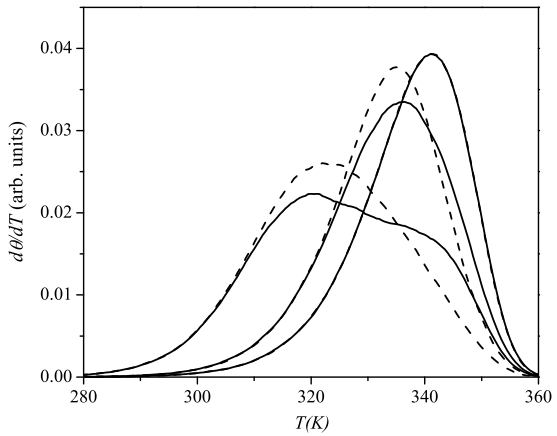

Fig. 5. Mobile (dash line) and immobile (line) as a function of temperature T for Inverse Relation spectra for TST dynamic with initial coverage $\theta_0 = 0.9$ and different values of the lateral interaction, left to right V (kcal/mol) $= 4, 0, -1$. For $V = 0$, mobile and immobile spectra coincide.

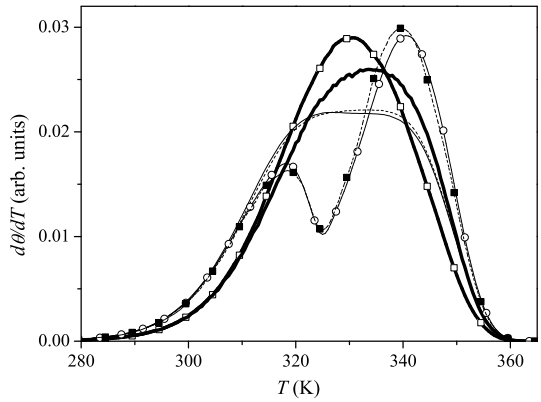

Fig. 6. Mobile (symbol) and immobile (line) TPD spectra as a function of temperature T for Soft Glauber Dynamic with initial coverage $\theta_0 = 0.9$ and different values of lateral interaction V (kcal/mol) $= 0$, (thick lines), 2 (dash lines), 4 (fine lines).

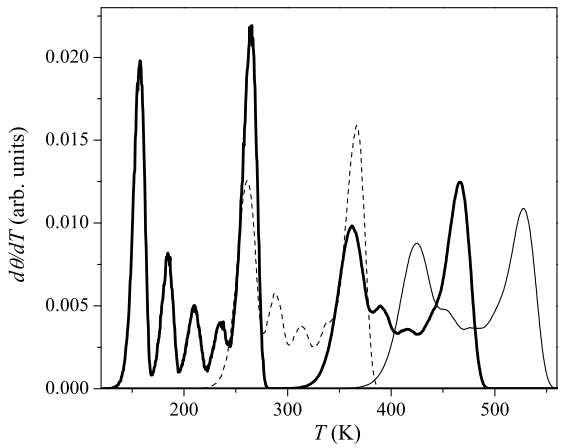

Fig. 7. Effect of energy barrier U on immobile TPD spectra as a function of temperature T for One-Step Dynamic with initial coverage $\theta_0 = 0.9$ and repulsive lateral interaction $V = 4$ kcal/mol, left to right U (kcal/mol) $= -6, 2, 10, 15$.

are more separated (and thus sharper) with increased the repulsive lateral interaction. The overtaking in temperature of the second peak of the spectrum with respect to the last peak of the immobile DTP is due to the fact that it is composed of particles that desorb with two, one and no first occupied neighbor, the system is not in the ordered phase and therefore

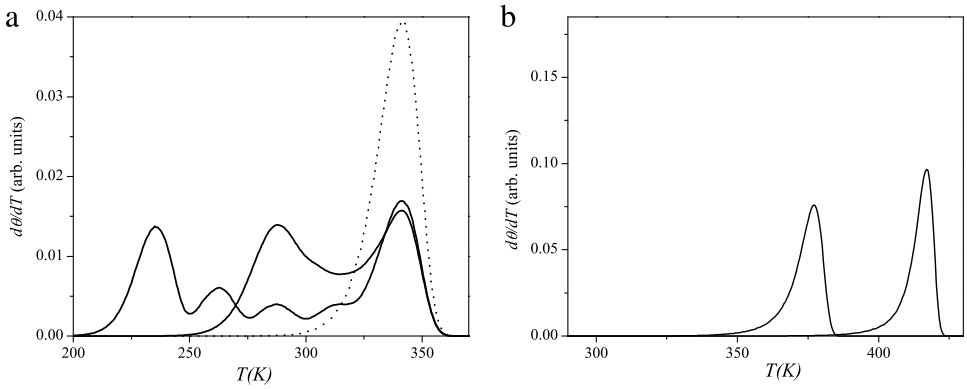

Fig. 8. Mobile (dash line) and immobile (line) TPD spectra as a function of temperature T for Ising kinetics with initial coverage $\theta_0 = 0.9$, TPD spectrum for $V = 0$ (dot line) is also include. (a) Repulsive lateral interaction, left to right V (kcal/mol) $= 2, 1, 0$; (b) Attractive lateral interaction, left to right V (kcal/mol) $= 0, -1, -2$.

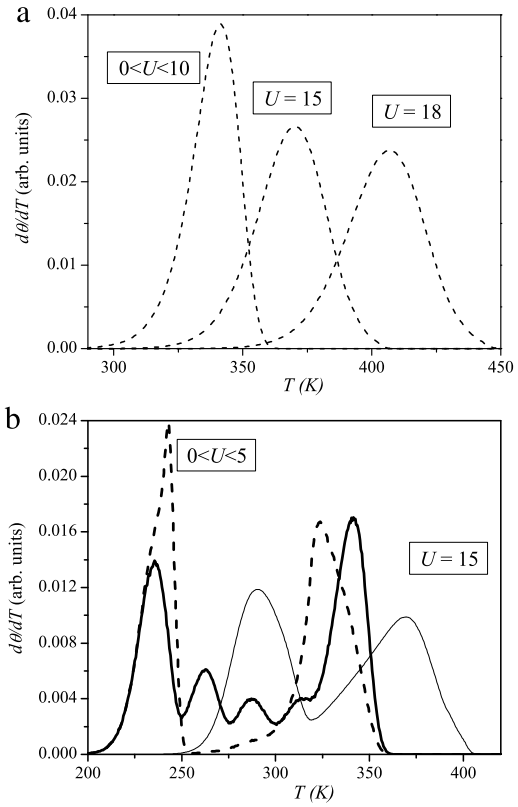

Fig. 9. Mobile (dash line) and immobile (line) TPD spectra as a function of temperature T for TDA with initial coverage $\theta_0 = 0.9$. (a) Non-interactive case $V = 0$, and different values of energy barrier U in kcal/mol; (b) Repulsive lateral interaction, $V = 2$ kcal/mol, and different values of U in kcal/mol.

the particles are not necessarily isolated. For mobile adsorbate, two peaks appear and the valley between them corresponds to the formation of the ordered phase $c(2 \times 2)$ (see Fig. 8(a)). Fig. 8(b) shows the DTPs for attractive lateral interactions, the system starts from an ordered structure formed by a large compact cluster. In the case of immobile spectra, the DTP is formed mainly by those particles that desorb having one and two occupied neighbors. Due to the presence of the ordered phase forced by the immobility of adsorbate, these particles are at the edge of the cluster. However, in the case of mobile spectra, the increase in temperature and mobility contribute to the disorder of the phase, due to that the desorption is composed by desorbed particles without occupied neighbors.

In Fig. 9 the DTP spectra for the kinetics of TDA are shown. It is interesting to analyze the effect of the value of the U parameter on the shape of TPD spectra. For a repulsive lateral interaction $V = 2$ kcal/mol the behavior of the spectrum

is similar to that of the Ising kinetics, however the increase of the U value impacts on the shape of the spectrum for the same interaction lateral, being also responsible for the drift of the DTP to higher temperatures, this shift of the spectrum is evidenced independently of the adsorbate mobility and both attractive and repulsive lateral interactions, with greater impact as the value of that parameter increases.

5. Conclusions

In this article, a study by Monte Carlo simulation on the influence of the different dynamic schemes proposed in adsorption–desorption kinetics applied to a two-dimensional system was presented.

The observables obtained with the soft dynamics have dissimilar behaviors, and sometimes are not consistent with the logical behavior for a lattice gas with nearest neighbor lateral interaction. In this sense, the TST has been the dynamic that best represents an adsorbed gas, showing that both the sticking coefficient and the TPD spectra give the same conclusion regarding the lateral interaction and the particle distribution for the system. As for the hard dynamics, the observables have a behavior similar to that of TST, with the exception of the sticking coefficient, which has a maximum between $0.5 < \theta < 1$ for repulsive lateral interactions, this effect is due to the dependence of the sticking coefficient respect to the chemical potential. That is, this behavior in sticking coefficient is indicative of the influence of the external field (gas pressure) on the system.

The choice of dynamics is arbitrary and only requires that the PDB be fulfilled. If, in addition, both members of the Eqs. (14)–(22) are positive, the same adsorption isotherms are obtained, regardless of the dynamics chosen. To analyze the dynamics, two other observables have been studied: sticking coefficient and TPD spectra. As shown in this article, this arbitrariness in the dynamic choice leads to that a given observable have different behaviors for the same value of lateral interaction. Some dynamics give anomalous behaviors in some cases, i.e. results that are not physically compatible with the value of the lateral interaction. Therefore, with a single observable it is not possible to determine the dynamics governing the processes of adsorption and desorption, and a careful analysis must be performed to determine the correct dynamic for each particular system.

Acknowledgment

This work was partially supported by the CONICET (Argentina).

References

[1] A. Cassuto, D.A. King, Surf. Sci. 102 (1981) 388.
[2] A. Córdoba, M.C. Lemos, J. Chem. Phys. 99 (1993) 4821.
[3] D. Grupta, C.S. Hirtzel Surf. Sci. 210 (1989) 322; Chem. Phys. Lett. 149 (1988) 527.
[4] C.B. Duke, E.W. Plummer (Eds.), Frontier in Surface and Interface Science, North-Holland, Amsterdam, 2002, pp. 84–172.
[5] G. Ertl, H. Knozinger, J. Weitkamp (Eds.), Handbook of Heterogeneous Catalysis, Wiley, New York, 1997.
[6] J.M. Heras, P.A. Velasco, L. Viscido, G. Zgrablich, Langmuir 7 (1991) 1124.
[7] Menzel, in: R. Gomer (Ed.), Interactions on Metal Surfaces, Springer-Verlag, Berlin, 1975, p. 102.
[8] V.P. Zhdanov, B. Kasemo, Chem. Phys. 177 (1993) 519 and references therein.
[9] Y.K. Tovbin, in: W. Rudzinski, A. Steele, G. Zgrablich (Eds.), Equilibria and Dynamics of Gas Adsorption on Heterogeneous Solid Surfaces, in: Studies in Surface Science and Catalysis, vol. 104, Elsevier, New York, 1997 and references therein.
[10] E.G. Seebauer, A.C.F. Kong, L.D. Schmidt, Surf. Sci. 193 (1988) 417.
[11] V.P. Zhdanov, K.I. Zarnaraev, Usp. Fiz. Nat. 149 (1986) 635; Sov. Phys.-Usp. 29 (1986) 7551.
[12] H.J. Kreuzer, Chem. Phys. 104 (1996) 9593.
[13] H.J. Kreuzer, Z.W. Gortel, Physisorption Kinetics, Springer-Verlag, Berlin, 1986.
[14] H.J. Kreuzer, S.H. Payne, Computational Methods in Colloid and Interface Science, Dekker, New York, 1999.
[15] J.H. Luscombe, Phys. Rev. B 29 (1984) 5128.
[16] S.H. Payne, H.J. Kreuzer, M. Kine, R. Denecke, H.-P. Steinrück, Surf. Sci. 513 (2002) 174.
[17] S.J. Manzi, V.J. Huespe, R.E. Belardinelli, V.D. Pereyra, Phys. Rev. E 80 (2009) 051112.
[18] V.P. Zhdanov, Elementary Physicochemical Processes on Solid Surfaces, Plenum, New York, 1991.
[19] G.M. Buendía, P.A. Rikvold, M. Kolesik, Phys. Rev. B 73 (2006) 045437; J. Mol. Struct.; Theochem. 769 (2006) 207.
[20] H.J. Kreuzer, J. Zhang, Appl. Phys. A Mater. Sci. Process. 51 (1990) 183.
[21] H.J. Kreuzer, S.H. Payne, Equilibria and dynamics of gas adsorption on heterogeneous solid surfaces, in: W. Rudzinski, W.A. Steele, G. Zgrablich (Eds.), Studies in Surfaces Science and Catalysis, Vol. 104, Elsevier, New York, 1997, p. 153 and references therein.
[22] A. Wierzbicki, H.J. Kreuzer, Surf. Sci. 257 (1991) 417.
[23] G. Costanza, S. Manzi, V.D. Pereyra, Surf. Sci. 524 (2003) 89.
[24] H.J. Kreuzer, S.H. Payne, Surf. Sci. 200 (1988) L433.
[25] H.J. Kreuzer, S.H. Payne, Surf. Sci. 198 (1988) 235.
[26] S.H. Payne, A. Wierzbicki, H.J. Kreuzer, Surf. Sci. 291 (1993) 242.
[27] S.H. Payne, H.J. Kreuzer, Surf. Sci. 205 (1988) 153.
[28] S.J. Manzi, G. Costanza y, V.D. Pereyra, Rev. Mex. Fís. 51 (1) (2005) 14.
[29] J.L. Sales, G. Zgrablich, Phys. Rev. B 35 (1987) 9520; Surf. Sci. 187 (1987) 1.
[30] S.J. Lombardo, A.T. Bell, Surf. Sci. Rep. 13 (1991) 3.
[31] M. Silverberg, A. Ben-Shaul, Surf. Sci. 214 (1989) 17.
[32] V.P. Zhdanov, Surf. Sci. 111 (1981) 63 111, (1981) L662; 123, (1982) 106; 133 (1983) 469; 157, (1985) L384; 165, (1986) L31; 171, (1986) L461; 209, (1989) 523.
[33] V.P. Zhdanov, Surf. Sci. Rep. 12 (1991) 185 and reference therein.
[34] V.D. Pereyra, G. Zgrablich, Langmuir 6 (1990) 118.

[35] V.D. Pereyra, G. Zgrablich, V.P. Zhdanov, Langmuir 6 (1990) 691.
[36] B. Li, C.-S. Zhang, V.P. Zhdanov, P.R. Norton, Surf. Sci. 322 (1995) 373.
[37] V.P. Zhdanov, B. Kasemo, Surf. Sci. 412 (1998) 527.
[38] R.A. van Santen, J.W. Niemantsverdriet, Chemical Kinetics and Catalysis, Plenum Press, New York, 1995.
[39] T. Ala-Nissila, S.C. Ying, Prog. Surf. Sci. 39 (1992) 227.
[40] T. Ala-Nissila, R. Ferrando, S.C. Ying, Adv. Phys. 51 (2002) 949.
[41] T. Ala-Nissila, J. Kjoll, S.C. Ying, Phys. Rev. B 46 (1992) 846.
[42] J.A. Boscoboinik, C. Plaisance, M. Neurock, W.T. Tysoe, Phys. Rev. B 77 (2008) 045422.
[43] F.M. Bulnes, V.D. Pereyra, J.L. Riccardo, Phys. Rev. E 58 (1998) 86.